Self-Stopping of Light

Mikhail Arkhipov[1], Rostislav Arkhipov[1,2] Ihar Babushkin[3,4,5] and Nikolay Rosanov[1,2]

[1]*St. Petersburg State University, Universitetskaya nab. 7/9, St. Petersburg 199034, Russia*
[2]*Ioffe Institute, Politekhnicheskaya strasse 26, St. Petersburg 194021, Russia*
[3]*Institute of Quantum Optics, Leibniz University Hannover, Welfengarten 1, 30167 Hannover, Germany*
[4]*Cluster of Excellence PhoenixD (Photonics, Optics, and Engineering—Innovation Across Disciplines),*
Welfengarten 1, 30167 Hannover, Germany
[5]*Max Born Institute, Max-Born-Strasse 2a, Berlin 10117, Germany*

Here, we show that light can bring itself to a complete standstill (self-stop) via self-interaction mediated by the resonant nonlinearity in a fully homogeneous medium. An intense few-cycle pulse, entering the medium, may reshape to form a strongly coupled light-matter bundle, in which the energy is transferred from light to the medium and back periodically on the single-cycle scale. Such oscillating structure can decelerate, alter its propagation direction, and even completely stop, depending on the state of its internal degrees of freedom. This phenomenon is expected to occur in the few-cycle strong-field regime when the Rabi oscillation frequency becomes comparable with the frequency of the incoming light.

Photons are particles which have zero rest mass and thus cannot be at rest. This is, however, formally not fully true for the light propagation in the medium, since the light-matter interaction creates "dressed photons," such as, for instance, polaritons—joint oscillations of light and collective atomic dipole [1–3]. These dressed photons are quasiparticles which do not have zero rest mass anymore. As any nonzero-mass particles, they may have zero velocity in a moving frame of reference, e.g., in a moving medium [4].

The group velocity of polaritonic wave packets can be very close to zero near resonances of the medium [3,5–7]. To mitigate the absorption, which unavoidably appears at resonances, specially designed multilevel systems exploiting so called electromagnetic induced transparency (EIT) [7] are used. Such EIT-based approaches allow us to achieve impressive slowing down [8,9] up to several meters per second [9]. Even more, the propagation can be completely stopped [10–12] if the pump in the EIT scheme is switched off, causing the polariton energy being stored in the atomic population wave packet.

Absorption near resonances can be avoided also using nonlinear light-matter interaction, namely so-called self-induced transparency (SIT) solitons, such as 2π solitons [13–21]. In a SIT soliton, the atomic ensemble makes a full Rabi oscillation over the pulse duration, so that the energy transferred to the matter and then fully returned back, so no overall losses occur. This results in a slowing down, which can be also very large for the long pulses. In "common" two-level atoms the velocity can never be zero [17,18,21], but this might be not true anymore for "artificial atoms," for instance ensembles of superconducting qubits [22].

In every case, we cannot expect that the velocity of very short, in particular, few-cycle pulses, can be significantly reduced using these methods. To make things worse, strong few-cycle pulses propagating in resonant media experience rather complex dynamics, including additional shortening and huge spectral shifts away from the resonance [23–25], to the frequencies which can be several times higher than the resonant frequency [24].

In this work, we show that slowing down, complete stop and even propagation direction reversal of a strong, single-cycle optical pulse is possible in a fully homogeneous resonant medium. The pulse is self-stopped in the course of relatively slow evolution due to highly nonlinear interaction of light with itself, mediated by the nonlinear medium. The evolution is accomplished by a formation of a novel localized structure, a dynamical, strongly coupled bundle of light and matter oscillating in time on a single-cycle scale with full exchange of energy between light and medium. This structure can stay or move with a speed of light depending just on its internal state, with the standing configuration being even energetically preferable over the moving one.

We describe propagation of light in a two-level resonant medium using the nonlinear wave equation [20,21] for the electric field $E(z,t)$ coupled to the Bloch equations [20,21] for the density matrix of two-level atoms ρ_{ij}, $\{i,j\} = \{1,2\}$:

$$\frac{d}{dt}\rho_{21}(z,t) = -\frac{\rho_{21}(z,t)}{T_2} + i\omega_{12}\rho_{12}(z,t) - \frac{id_{12}}{\hbar}n(z,t)E(z,t),$$

$$\frac{d}{dt}n(z,t) = -\frac{n(z,t)-n_0}{T_1} + \frac{4d_{12}E(z,t)}{\hbar}\text{Im}[\rho_{12}(z,t)], \quad (2)$$

$$\frac{\partial^2 E(z,t)}{\partial z^2} - \frac{1}{c^2}\frac{\partial^2 E(z,t)}{\partial t^2} = \frac{4\pi}{c^2}\frac{\partial^2 P(z,t)}{\partial t^2}. \tag{3}$$

Here, $n = \rho_{11} - \rho_{22}$ describes the population inversion, $n_0(z,t) = 1$ is its value at the equilibrium, ω_{12}, d_{12}, T_1, T_2 are the transition frequency, dipole moment, the population, and polarization relaxation times respectively, $\hbar$ is the reduced Plank constant, c is the speed of light in vacuum, $P(z,t) = 2N_0 d_{12}\mathrm{Re}\rho_{12}$ is the atomic polarization, N_0 is the concentration of the two-level atoms. Neither slowly varying envelope approximation nor rotating wave approximation are used in Eqs. (1)–(3), allowing us to model pulses of arbitrary wave shape. Equations (1)–(3) are widely used to study the coherent propagation of few-cycle pulses in resonant media in different cases, including SIT [24–34]. These equations were solved by the finite-difference method coupled to the fourth order Runge-Kutta method [35]. For the discussion of the generality of these equations and possible materials to use see Supplemental Material [36].

For the simulations, we assume the following parameters for the medium: layer length 3.2 μm, $d_{12} = 5$ D, $T_1 = 1$ ps, $T_2 = 20$ fs, $\omega_{12} = 2.69$ rad/fs, corresponding to the transition wavelength $\lambda_{12} = 700$ nm, $N_0 = 6.3 \times 10^{22}$ cm^{-3}. The initial pulse shape is given by

$$E(0,t) = E_0 \exp\left(-t^2/\tau^2\right)\sin\left[\omega_0 t\right], \tag{4}$$

with the pulse duration $\tau = 2.33$ fs, central frequency $\omega_0 = \omega_{12}$, and peak field amplitude $E_0 = 1.656 \times 10^6$ ESU.

The results of numerical simulations for those parameters are shown in Fig. 1. It is seen that directly after the entrance the field and inversion form an oscillating structure, which starts to decelerate and is fully stopped at $z \approx 8\lambda_{12}$. The total energy in field $\mathcal{E}(t) \propto \int E^2(z,t)dz$ oscillates quickly in time Fig. 1(c). The character of propagation and dynamics of $\mathcal{E}(t)$ indicate three different stages of evolution: at $t \approx t_1 = 18$ fs fast oscillations of $\mathcal{E}(t)$ are born; for $t_1 \lesssim t \lesssim t_2 = 45$ fs the average amount of energy in the pulse remains approximately the same whereas the pulse decelerates and stops; finally, for $t \gtrsim t_2$ the pulse remains standing whereas its energy $\mathcal{E}$ quickly drops with time (nevertheless, the structure remains visible and standing for remarkably extended time $\gtrsim 100$ fs, see Supplemental Material [36]).

This general behavior is quite stable and can be reproduced for a broad range of the input pulse parameters. In particular, in Fig. 1(c) (black line) we show the transmitted power fraction $W_{\mathrm{out}}/W_{\mathrm{in}}$ [here $W(z) = \int E^2(z,t)dt$ and W_{out} and W_{in} refer to the values of W at the entrance and at the output of the medium] vs the atomic density. Small values of $W_{\mathrm{out}}/W_{\mathrm{in}}$ indicate that the light is trapped inside the medium. We also see that the trapping z position changes with N_0 [orange curve in Fig. 1(c)]. More examples for different parameters can be found in Supplemental Material [36] and visualizations [40–42].

The spectrum [Figs. 1(e) and 1(f)] experiences significant modification already soon after the entrance, well before the self-stop occurs. In particular, in the region between the entrance $z = 5.27\lambda_{12}$ and $z \approx 6\lambda_{12}$ the
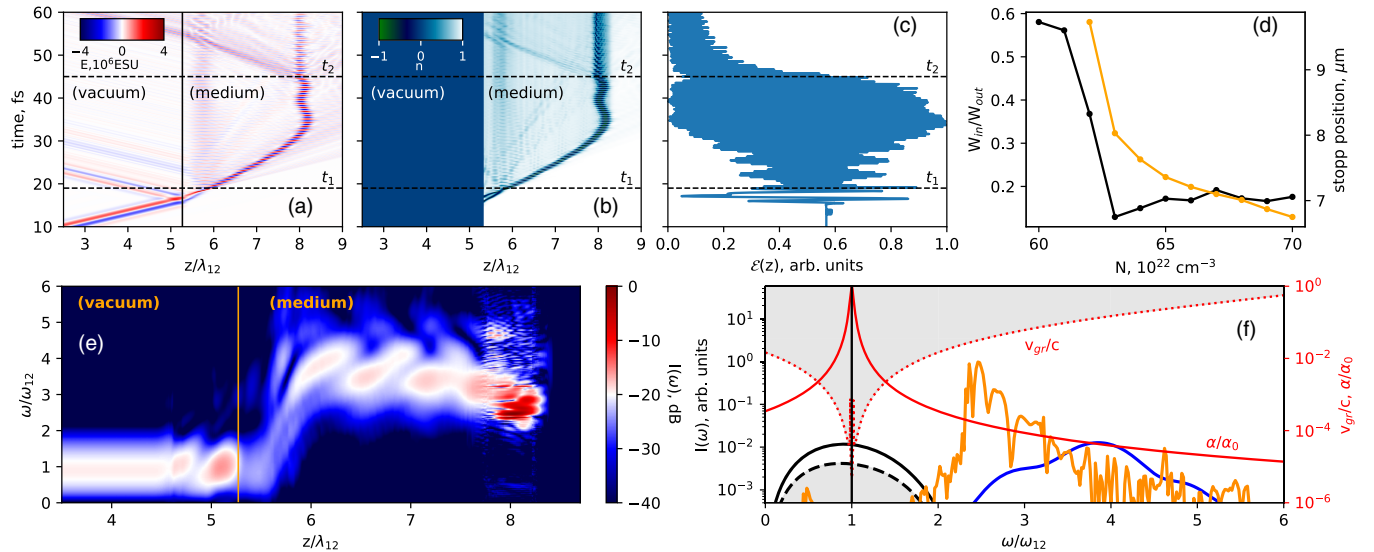

FIG. 1. Self-stopping light. (a),(b) Evolution of the field $E(z,t)$ (a) of a short pulse entering a resonant medium, and its inversion $n(z,t)$ (b). After a reach transient dynamics the light self-stops at around $z \approx 8\lambda_{12}$. The points t_1 and t_2 indicate quantitative changes in the dynamical regime. (c) Dynamics of the energy in the field $\mathcal{E}(t)$. (d) The transmitted light fraction $W_{\mathrm{out}}/W_{\mathrm{in}}$ (black line) and the position of the stop point (orange line) as a function of the particle density N_0. (e) Evolution of the field spectrum $I(z,\omega)$ with z. (f) Spectra $I(z,\omega)$ at certain z positions: solid black line: $z = 4\lambda_{12}$ (before the entrance); solid blue line: $z = 6.2\lambda_{12}$; solid orange line $z = 8\lambda_{12}$. For comparison, also the spectrum of a conventional SIT soliton (black dashed curve), as well as the linear losses α (red solid line) normalized to the maximum α_0 and the linear group velocity $v_{\mathrm{gr}}(\omega)$ (red dotted curve) in units of c for the small-signal situation are presented.

spectrum experiences a quick dramatic shift from ω_{12} to around $4\omega_{12}$, after which it slowly moves down to around $2.5\omega_{12}$. Such shifts were observed before in [23,24] and are typically related to the pulse shortening dynamics. Importantly, the strong spectral shifts make our pulse strongly nonresonant already close to the entrance, which alone makes it fundamentally different from the common EIT- and SIT-based pulses, which are always pinned to the resonance. Also, the pulse velocity is fully incompatible with the one imposed by both the SIT soliton velocity and the group velocity $v_{\mathrm{gr}}(\omega) = d\omega/dk$ dictated by the dispersion curve $k(\omega)$ shown in Fig. 1(f) and thus with the EIT mechanism (see Supplemental Material [36] for more details).

As one can see, the pulse shape also significantly changes already soon after entering the medium. In Fig. 2 we consider in more detail this initial stage of evolution around $t \approx t_1$. Two half-waves of the initial pulse approach each other and "collide" [Figs. 2(a)–2(c)], resulting in a stable solitary structure, which not only propagates in space but also quickly oscillates in time with the half-period $T \approx 0.44$ fs. A half-period of such oscillation is shown in Figs. 2(d)–2(f). This dynamics is very much different from a typical SIT soliton propagation, which is

shown for comparison in Figs. 2(g) and 2(h). The latter is obtained from an input pulse with the same parameters except E_0 which is in that case is 1.36 times larger, and results in two independent 2π SIT solitons propagating unchanged and with a constant velocity.

Therefore, we observe here a novel highly oscillating solitary structure which we call a light-matter oscillon (LMO). The term oscillon is often used to describe oscillating solitary or close to solitary solutions in different areas of physics [43–47]. In contrast to a SIT soliton, the energy $\mathcal{E}(t)$ of LMO oscillates periodically in time, indicating energy transfer between matter and light [see Fig. 2(i)]. The relations between oscillations of E, P, and n in time are very different between the LMO and SIT [cf. Fig. 2(e) and inset to Fig. 2(i)]. In contrast to SIT, E and P oscillate in antiphase, whereas n oscillates twice as fast as E and has a phase shift $\pi/2$ to E, performing thus oscillations $-E \to n \to E \to n \to \cdots$ which half-period we denote as T.

The stopping process of LMO is detailed in Fig. 3. In the region between ≈ 30 and ≈ 45 fs, the velocity of LMO quickly decreases, performing yet several relatively slow oscillations [Figs. 3(a)–3(c) and Fig. 4] whereas the fast oscillations discussed above retain its period mostly
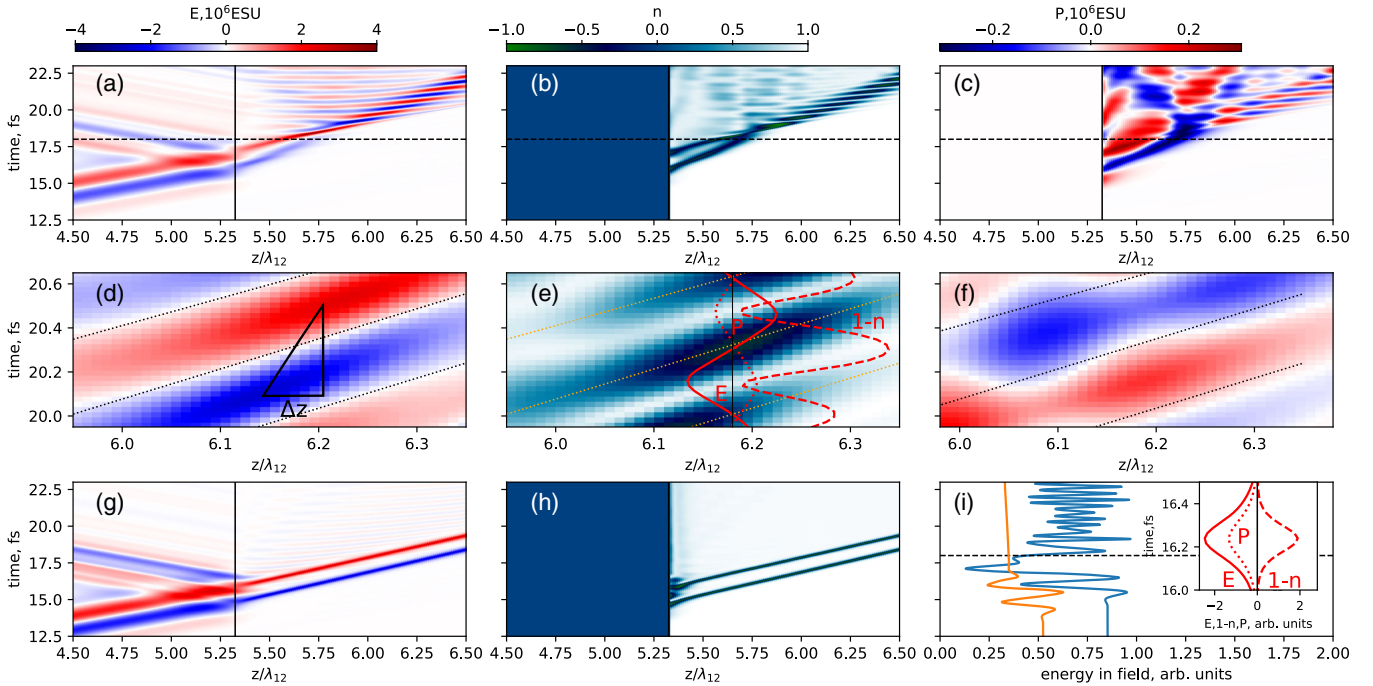

FIG. 2.   Formation of LMO near the entrance to the medium. (a)–(f) Evolution of the field (a), inversion (b), and atomic polarization (c) on the scale of multiple (a)–(c) and half (d)–(f) of period of LMO oscillation. Horizontal line in (a)–(c),(i) marks $t = 18$ fs as the position where the collapse takes place and LMO is born. In (d)–(f), dashed lines indicate zeros of $E(z,t)$. The consequent half-oscillations of the field are displaced by Δz in space. For comparison, in (g),(h) the evolution of a more conventional SIT soliton structure (two copropagating 2π solitons) is shown. (i) The dynamics of the energy in field $\mathcal{E}(t)$ for LMO (blue line) and the SIT soliton (orange line). Inset in (i) shows the field (red solid line) inversion (red dashed line) and atomic polarization (red dotted line) in dependence on time for one of the SIT solitons at $z = 5.8$ μm. In (e), red lines show the time dependence of the field, polarization and inversion for $z = 6.18$ μm [to be compared with the SIT soliton case in (i)].
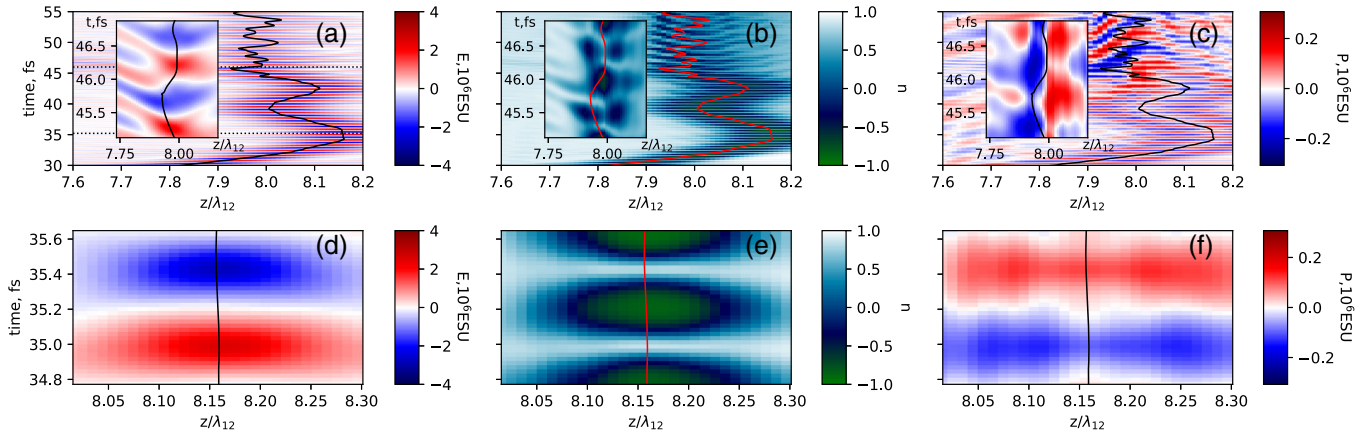
FIG. 3.   Details of LMO self-stopping dynamics. (a)–(c) The dynamics of the field (a), inversion (b), and atomic polarization (c) in the range where it self-stops. (d)–(f) and insets to (a)–(c) show the dynamics of E, n, and P on the single-cycle scale near exemplary time positions marked in (a) by dotted horizontal lines [$t \approx 35$ fs (d)–(f) and $t \approx 46$ fs [insets to (a)–(c)]. Solid lines in (a)–(f) show the evolution of the center of mass (CM) of the field.

unchanged. We observe, however, that the basic structure of the oscillation cycle of LMO is somewhat modified. Whereas in the beginning of the propagation Fig. 2(d) every (half-)oscillation in time is accomplished by the shift in z by Δz, at the position when the structure stopps, Δz approaches zero Fig. 3(d). This leads us to the following understanding of the dynamics (see also Fig. 4): the "perfect," "ideal" LMO has $\Delta z = 0$ and does not move (its velocity $v = 0$). In the collapse event at the beginning of propagation a "deformed" LMO is born, with $\Delta z \neq 0$. Because of this, by every oscillation half-period T in time the structure advances by Δz in space. The velocity of the structure must be thus $v = \Delta z / T$. This is supported by Fig. 4(b) where the velocity v computed via the evolution of the center of mass (CM) of the pulse is compared with the velocity given by $\Delta z / T$. Furthermore, we observe [see Fig. 4(a)] that the "diffractive" energy of the field $H_{\text{diff}} \propto \int (\partial_z E)^2 dz$ (see more detailed definition in Supplemental Material [36]) is higher for the deformed structure with $\Delta z \neq 0$ than for the nondeformed one. This leads to an effective potential $H_{\text{eff}} \propto a' \Delta z^2$, giving, from H_{diff} [see Fig. 4(a)], the oscillation frequency $o' \approx 0.9$ rad/fs. This fits well to the dynamics of Δz as shown in Fig. 4(b) where oscillations of Δz are obtained with a pendulum model with energy H_{eff}, additionally modified by a phenomenological nonlinear nonpotential term to take into account corrections at large Δz (see Supplemental Material [36] for details). Thus, we conclude that oscillations of the velocity we observe in Figs. 3(a)–3(c) and Fig. 4(b) for $t \lesssim 46$ fs are indeed relaxation oscillations bringing the deformed LMO ($\Delta z \neq 0$) to its nondeformed state ($\Delta z = 0$).

As the system approaches $\Delta z = 0$ close enough (at $t \approx t_2 \approx 49$ fs), its dynamics is modified once more. Although the basic LMO structure still remains (fast oscillations $E \rightarrow n \rightarrow -E \rightarrow \cdots$) its internal spatiotemporal structure becomes significantly more complex as seen in
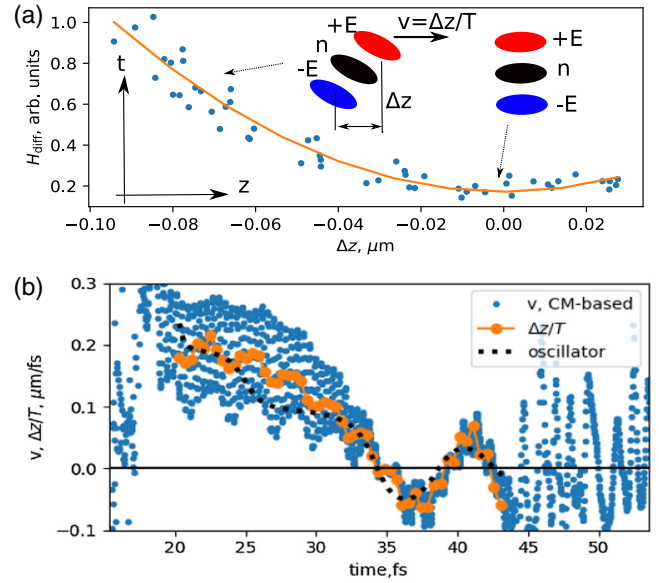

FIG. 4.   Self-stopping of LMO as a relaxation to the energy minimum. (a) The dependence of the diffractive energy H_{diff} of LMO in dependence on the displacement Δz. Dots show the numerically calculated energies for every particular oscillation tracked along the position of CM in Fig. 3, the solid orange line shows the quadratic fit to the data points. The insets show the undeformed LMO ($\Delta z = 0$, having the minimal energy) as well as deformed LMO ($\Delta z \neq 0$, out of the energy minimum) advancing by Δz every half-period T and thereby moving, at the same time slowly relaxing to the minimum and thus to the undeformed structure. (b) Blue dots: velocity v of LMO calculated from the CM curve in Fig. 3; orange circles: the velocity suggested from the displacement as $v = \Delta z / T$. Black dots indicate the fit to the relaxation dynamics obtained from the oscillator model following from the potential in (a) as described in text.

the insets to Figs. 3(a)–3(c), the overall CM movement acquires fast quasiperiodic oscillations and the energy starts to dissipate quickly [Fig. 1(c)], mainly due to the radiative losses. Despite this, this more complex structure remains standing on average until it is fully radiated away [see Figs. 1(a) and 1(b) and Supplemental Material [36]].

Finally, we find that the basic, undeformed ($\Delta z = 0$) LMO can be described analytically. Here, we only sketch the derivation, with more details given in Supplemental Material [36]. First, neglecting the z dependence and relaxation times in Eqs. (1) and (2), we obtain $E = -4\pi P$ and thereby can solve Eq. (2), getting $N = N_0 + (4\pi/\hbar\omega_{12})P^2$. These expressions show that E oscillates in antiphase to P and N is two times faster than E and P thus giving the key features of LMO [cf. Fig. 2(e)]. Furthermore, substituting this formula back to the equation for P, we obtain the equation for an anharmonic oscillator $\ddot{E} + a^2 E + bE^3 = 0$, $a^2 = \omega_{12}^2 + (8\pi\omega_{12}d_{12}^2/\hbar)N_0$, $b = (2d_{12}^2/\hbar^2)$, which, as known, have periodic solutions with the frequency which in the first approximation is given by $\omega = \sqrt{\omega_{12}^2 + (8\pi\omega_{12}d_{12}^2N_0/\hbar) + (3/2)\Omega_R^2}$, where Ω_R is the Rabi frequency, giving $\omega/\omega_{12} \approx 5$ for our parameters, which is of the same order as the numbers we see in Figs. 1(e) and 1(f).

In conclusion, we predict the existence of a novel ultrashort structure, light-matter oscillon, in which light and matter form a tightly connected bundle, oscillating on the single-cycle scale. Self-stopping occurs because of the slow evolution of the internal degree of freedom, the displacement Δz, toward the energy minimum. It is a fundamentally nonlinear self-interaction phenomenon, in a strong-field single-cycle regime, thus in a certain sense opposite to EIT or SIT, based on the resonant, long-pulse dynamics.

[1] A. Rahimi-Iman, *Polariton Physics* (Springer, New York, 2020), 229.

[2] P. Törmä and W. L. Barnes, Strong coupling between surface plasmon polaritons and emitters: A review, Rep. Prog. Phys. **78**, 013901 (2015).

[3] M. Fleischhauer and M. D. Lukin, Dark-State Polaritons in Electromagnetically Induced Transparency, Phys. Rev. Lett. **84**, 5094 (2000).

[4] O. Kocharovskaya, Yu. Rostovtsev, and M. O. Scully, Stopping Light via Hot Atoms, Phys. Rev. Lett. **86**, 628 (2001).

[5] E. B. Aleksandrov and V. S. Zapasskii, A fairy tale of stopped light, Phys. Usp. **47**, 1033 (2004).

[6] R. W. Boyd, Slow and fast light: Fundamentals and applications, J. Mod. Opt. **56**, 1908 (2009).

[7] S. E. Harris, Electromagnetically induced transparency, Phys. Today **50**, No. 7, 36 (1997).

[8] M. M. Kash, V. A. Sautenkov, A. S. Zibrov, L. Hollberg, G. R. Welch, M. D. Lukin, Yu. Rostovtsev, E. S. Fry, and M. O. Scully, Ultraslow Group Velocity and Enhanced Nonlinear Optical Effects in a Coherently Driven Hot Atomic Gas, Phys. Rev. Lett. **82**, 5229 (1999).

[9] L. V. Hau, S. E. Harris, Z. Dutton, and C. H. Behroozi, Light speed reduction to 17 metres per second in an ultracold atomic gas, Nature (London) **397**, 594 (1999).

[10] D. F. Phillips, A. Fleischhauer, A. Mair, R. L. Walsworth, and M. D. Lukin, Storage of Light in Atomic Vapor, Phys. Rev. Lett. **86**, 783 (2001).

[11] Ch. Liu, Z. Dutton, C. H. Behroozi, and L. V. Hau, Observation of coherent optical information storage in an atomic medium using halted light pulses, Nature (London) **409**, 490 (2001).

[12] N. S. Ginsberg, Ch. Slowe, and L. V. Hau, Coherent control of optical information with matter wave dynamics, Nature (London) **445**, 623 (2007).

[13] S. L. McCall and E. L. Hahn, Self-induced transparency, Phys. Rev. **183**, 457 (1969).

[14] H. M. Gibbs and R. E. Slusher, Peak Amplification and Breakup of a Coherent Optical Pulse in a Simple Atomic Absorber, Phys. Rev. Lett. **24**, 638 (1970).

[15] M. J. Ablowitz, D. J. Kaup, and A. C. Newell, Coherent pulse propagation, a dispersive, irreversible phenomenon, J. Math. Phys. (N.Y.) **15**, 1852 (1974).

[16] I. P. Gabitov, V. E. Zakharov, and A. V. Mikhailov, Nonlinear theory of superfluorescence, Zh. Exp. Theor. Phys. **86**, 1204 (1984), http://jetp.ras.ru/cgi-bin/e/index/r/86/4/p1204?a=list.

[17] G. L. Lamb, Jr., Phase Variation in Coherent-Optical-Pulse Propagation, Phys. Rev. Lett. **31**, 196 (1973).

[18] G. L. Lamb, Jr., Analytical descriptions of ultrashort optical pulse propagation in a resonant medium, Rev. Mod. Phys. **43**, 99 (1971).

[19] N. L. Komarova and A. C. Newell, The competition between nonlinearity, dispersion and randomness in signal propagation, IMA J. Appl. Math. **63**, 267 (1999).

[20] L. Allen and J. H. Eberly, *Optical Resonance and Two-Level Atoms* (Courier Corporation, New York, 1987), Vol. 28.

[21] A. Yariv, *Quantum Electronics* (Wiley, New York, 1989).

[22] Z. Ivić, N. Lazarides, and G. P. Tsironis, Self-induced transparency in a flux-qubit chain, Chaos, Solitons Fractals X **1**, 100003 (2019).

[23] V. P. Kalosha and J. Herrmann, Formation of Optical Subcycle Pulses and Full Maxwell-Bloch Solitary Waves by Coherent Propagation Effects, Phys. Rev. Lett. **83**, 544 (1999).

[24] R. Arkhipov, M. Arkhipov, A. Demircan, U. Morgner, I. Babushkin, and N. Rosanov, Single-cycle pulse compression in dense resonant media, Opt. Express **29**, 10134 (2021).

[25] R. Arkhipov, M. Arkhipov, I. Babushkin, A. Pakhomov, and N. Rosanov, Coherent propagation of a half-cycle unipolar attosecond pulse in a resonant two-level medium, J. Opt. Soc. Am. B **38**, 2004 (2021).

[26] S. Hughes, Breakdown of the Area Theorem: Carrier-Wave Rabi Flopping of Femtosecond Optical Pulses, Phys. Rev. Lett. **81,** 3363 (1998).

[27] D. V. Novitsky, Propagation of subcycle pulses in a two-level medium: Area-theorem breakdown and pulse shape, Phys. Rev. A **86,** 063835 (2012).

[28] R. M. Arkhipov, M. V. Arkhipov, I. Babushkin, A. Demircan, U. Morgner, and N. N. Rosanov, Ultrafast creation and control of population density gratings via ultraslow polarization waves, Opt. Lett. **41,** 4983 (2016).

[29] R. M. Arkhipov, A. V. Pakhomov, M. V. Arkhipov, I. Babushkin, A. Demircan, U. Morgner, and N. N. Rosanov, Population density gratings induced by few-cycle optical pulses in a resonant medium, Sci. Rep. **7,** 12467 (2017).

[30] N. V. Vysotina, N. N. Rozanov, and V. E. Semenov, Extremely short pulses of amplified self-induced transparency, JETP Lett. **83,** 279 (2006).

[31] N. N. Rosanov, V. E. Semenov, and N. V. Vysotina, Few-cycle dissipative solitons in active nonlinear optical fibres, Quantum Electron. **38,** 137 (2008).

[32] N. V. Vysotina, N. N. Rosanov, and V. E. Semenov, Extremely short dissipative solitons in an active nonlinear medium with quantum dots, Opt. Spectrosc. **106,** 713 (2009).

[33] V. V. Kozlov, N. N. Rosanov, and S. Wabnitz, Obtaining single-cycle pulses from a mode-locked laser, Phys. Rev. A **84,** 053810 (2011).

[34] Y. Y. Lin, I-H. Chen, and R.-K. Lee, Few-cycle self-induced-transparency solitons, Phys. Rev. A **83,** 043828 (2011).

[35] A. Taflove and S. C. Hagness, *Computational Electrodynamics: The Finite-Difference Time-Domain Method* (Artech House, Boston, London, 2005).

[36] See Supplemental Material at http://link.aps.org/supplemental/10.1103/PhysRevLett.128.203901, which includes Refs. [37–39].

[37] O. D. Mücke, T. Tritschler, M. Wegener, U. Morgner, and F. X. Kärtner, Signatures of Carrier-Wave Rabi Flopping in GaAs, Phys. Rev. Lett. **87,** 057401 (2001).

[38] J. Ryou, Y. S. Kim, K. C. Santosh, and K. Cho, Monolayer MoS_2 bandgap modulation by dielectric environments and tunable bandgap transistors, Sci. Rep. **6,** 29184 (2016).

[39] L. Yuan, W. Hu, H. Zhang, L. Chen, and Q. Wang, Cu_5FeS_4 nanoparticles with tunable plasmon resonances for efficient photothermal therapy of cancers, Front. Bioeng. Biotechnol. **8,** 21 (2020).

[40] Visualization 1 of the field, polarization, and inversion, for the parameters of Figs. 1–3.

[41] Visualization 2 of the field, polarization, and inversion for the same parameters but $N_0 = 6.1 \times 10^{22}$ cm^{-3}.

[42] Visualization 3 of the field, polarization, and inversion for the same parameters but $\omega_0 = 3\omega_{12}$ (making the input pulse nonresonant and containing several cycles instead of only one).

[43] E. Clément, L. Vanel, J. Rajchenbach, and J. Duran, Pattern formation in a vibrated granular layer, Phys. Rev. E **53,** 2972 (1996).

[44] P. B. Umbanhowar, F. Melo, and H. L. Swinney, Localized excitations in a vertically vibrated granular layer, Nature (London) **382,** 793 (1996).

[45] H. Arbell and J. Fineberg, Temporally Harmonic Oscillons in Newtonian Fluids, Phys. Rev. Lett. **85,** 756 (2000).

[46] R. E. Noskov, P. A. Belov, and Y. S. Kivshar, Sub-wavelength Modulational Instability and Plasmon Oscillons in Nanoparticle Arrays, Phys. Rev. Lett. **108,** 093901 (2012).

[47] G. Fodor, P. Forgács, Ph. Grandclément, and I. Rácz, Oscillons and quasibreathers in the ϕ^4 Klein-Gordon model, Phys. Rev. D **74,** 124003 (2006).